7. Glyva, V. A. Rozroblennia i doslidzhennia kompozytnykh elektrpmagnitnykh ekraniv z kerovanymy zakhysnymy vlastyvosniamy [Text] / V. A. Glyva, I. M. Podobied, O. L. Matvieieva // Visnyk NTUU «KPI». Seriia «Girnytstvo». – 2011. – Issue 21. – P. 176–181.
8. Patil, N. Electric, magnetic and high frequency properties of screen printed ferrite-ferroelectric composite thick films on alumina substrate [Text] / N. Patil, N. B. Velhal, R. Pawar, V. Puri // Microelectronics International. – 2015. – Vol. 32, Issue 1. – P. 25–31. doi: 10.1108/mi-12-2013-0080
9. Fionov, A. S. Polymer nanocomposites: synthesis and physical properties [Text] / A. S. Fionov, G. Y. Yurkov, O. V. Popkov, I. D. Kosobudskii, N. A. Taratanov, O. V. Potemkina // Advances in Composite Materials or Medicine and Nanotechnology. – 2011. – P. 343–364. doi: 10.5772/14881
10. Ceken, F. Electromagnetic Shielding Properties of Plain Knitted Fabrics Containing Conductive Yarns [Text] / F. Ceken, G. Pamuk, A. Ozkurt, S. Ugurlu // Journal of Engineered Fibers and Fabrics. – 2012. – Vol. 7, Issue 4. – P. 81–87.
11. Bychkov, I. V. Isledovanie prohozhdeniia I otrazheniia SVCH izlucheniia v mnogosloinyh kompozitnyh materialah $CaS0_4{\cdot}2H_2O$ – grafit [Text] / I. V. Bychkov, I. S. Zotov, A. A. Fedii // Pisma v zhurnal teoreticheskoi fiziki. – 2011. – Vol. 37, Issue 14. – P. 90–94.
12. Taranov, N. A. Sintez reniisoderzhashchih nanochastits na poverhnosti mikrogranul politetraftoretilena [Text] / N. A. Taranov, G. Yu. Yurkov, I. D. Kosobudskyi // Vestnik Saratovskogo gosudarstvennogo tehncheskogo universiteta. – 2010. – Issue 44. – P. 95–101.
13. Bhattacharjee, S. Protective Measures to Minimize the Electromagnetic Radiation [Text] / S. Bhattacharjee // Electronic and Electric Engineering. – 2014. – Vol. 4, Issue 4. – P. 375–380.
14. Dengub, V. I. Determination of fiber filter dust collecting efficiency depending on particles distribution of industrial dust [Text] / V. I. Dengub, V. A. Shapovalov, N. V. Hudyk // Metallurgical and Mining Industry. – 2015. – Issue 5. – P. 67–71. – Available at: http://www.metaljournal.com.ua/assets/MMI_2014_6/MMI_2015_5/010Hudyk.pdf

Наведено результати досліджень механізму прямого і зворотного мартенситного перетворення в поверхневому шарі шліфований деталі із загартованої сталі. Показано, що при шліфуванні в основному має місце зворотне мартенситне перетворення за схемою мартенсит – перліт –аустеніт. Показана можливість швидкісного відпустки мартенситу до перліту, під дією контактної температури шліфування, який при подальшому підвищенні температури перетворюється в аустеніт, утворюючи припік гарту

Ключові слова: мартенситних перетворення, контактна температура, швидкість на гріву, відпустка мартенситу, швидкість дифузії, температура аустенітизації

Приведены результаты исследований механизма прямого и обратного мартенситного превращения в поверхностном слое шлифуемой детали из закаленной стали. Показано, что при шлифовании в основном имеет место обратное мартенситное превращение по схеме мартенсит – перлит –аустенит. Показана возможность скоростного отпуска мартенсита до перлита, под действием контактной температуры шлифования, который при дальнейшем повышении температуры превращается в аустенит, образуя прижёг закалки

Ключевые слова: мартенситное превращение. контактная температура, скорость нагрева, отпуск мартенсита, скорость диффузии, температура аустенитизации

UDC 621.923-5
DOI: 10.15587/1729-4061.2017.103149

MARTENSITE TRANSFORMATIONS IN THE SURFACE LAYER AT GRINDING OF PARTS OF HARDENED STEELS

V. Lebedev
Doctor of Technical Sciences, Professor*
E-mail: wlebedev29@rambler.ru
N. Klimenko
PhD, Associate Professor*
I. Uryadnikova
PhD, Associate Professor
The State Emergency Service of Ukraine
Rybalska str., 18, Kyiv, Ukraine, 01011
E-mail: ingavictory@gmail.com
T. Chumachenko
PhD, Associate Professor*
A. Ovcharenko
Postgraduate student*
E-mail: ovcharenko-a.v@ro.ru
*Department of Structural Materials Technology and Materials
Odessa National Polytechnic University
Shevchenko ave., 1, Odessa, Ukraine, 65044

1. Introduction

Most often, thermal grinding defects are formed in cemented, improved high-carbon, low and medium-alloyed steels with a martensite or tempered martensite structure [1–3]. When the surface of the part of the hardened steel is rapidly heated by the grinding temperature above the Ac_1 line, the martensitic structure of the surface layer transforms

into an austenitic structure, that is, an inverse martensitic transformation takes place. This transformation is all the more facilitated by the fact that as a result of the high specific pressures exerted by the abrasive grains on the surface of the metal, the Ac_1 point is shifted to a region of lower temperatures [2, 4, 5].

After the rapid heating of the surface layer, rapid cooling follows at rates much higher than the critical quenching rates. The M_f points for these steels are mostly below 20 °C, that is, below the temperature to which the metal is cooled during grinding. As a result, martensitic transformations do not take place completely, due to which a structure of austenite of secondary hardening is fixed in the surface layer, called the grinding hardening quench.

The final cooling of the austenite structure occurs in the temperature range from 20 °C and lower. The cooling process ends between the M_s and M_f points. The temperature interval until the end of the martensitic transformation does not overlap, which causes incompleteness of this transformation and fixation of a significant part of the austenite.

Phase-structural changes in the surface layer of hardened steel during grinding are called grinding burns. Burns cause high residual stresses and cracks in the surface layer, a decrease in wear resistance of the ground surface. This reduces the strength, reliability and durability of the ground surface, and, consequently, of the entire part [3, 5].

At present, there are many new low and high-alloy steels that are widely used for surfacing the working surfaces of parts that need to be ground. In view of this, there is a need to determine safe grinding temperatures, which do not lead to grinding defects in the surface layer. These temperatures can be determined using an analytical study of the kinetics of phase-structural transformations during grinding.

In all these cases, the surface layer of the working surfaces of such parts is very sensitive to the grinding temperatures, which cause grinding burns.

This issue needs further clarification, since it is very relevant for machine building, especially for gas turbine construction, where it is necessary to grind thoroughly the reduction gear wheels.

2. Literature review and problem statement

The values of the critical temperatures that cause thermal defects are discussed in sufficient detail in [6–8]. However, in the first two papers, the analysis is not related to grinding. They consider relatively low heating and cooling rates, which does not allow the results to be interpreted from the point of view of grinding. In the third paper, modeling using laser heating is used, which leads the author to the erroneous idea that with an increase in the heating rate, critical temperatures decrease, so these results can not be used when considering the heating kinetics during grinding.

The papers [1, 2] consider the issue and conclusions of an adequate reflection of real processes rather deeply, however, these results need clarification and some simplification to be used in the practice of the shops of machine-building enterprises.

In [9], the mechanism of austenite-martensite transformations hereinafter abbreviated as A–M, depending on the size of the metal grains in repeated rapid heating is investigated and the possibilities of forming brittle and plastic structures are explored. Despite the fact that the researchers use high-speed heating, the experimental conditions are not adequate to the conditions of heating during grinding and the results cannot be used.

In [10], a kinetic model is studied to understand the martensite – austenite transformation, hereinafter abbreviated as M–A, in cold – rolled steel, and then annealed metastable austenite in ultra fine-grained steel. However, in this paper, the conditions are studied that facilitate this transformation from the point of view of the need of plastic deformation and the presence of nitrogen in the intercrystalline space. This does not correspond to the conditions available for grinding.

In [11], the influence of high-density energy sources on morphological changes in steel investigated by physical imitation. Carbon steel strips were subjected to thermal cycles to temperatures from 400 to 1200°C, followed by cooling in water. The thermal cycles provided a heating rate of up to 1000°C, continuous austenitization was investigated, and the results were checked by microhardness measurements. It was found that complete austenitization during the M–A transformation occurs at temperatures above Ac_3. results of research, with regard to transformations in grinding, must be treated with great care. The heating rates are significantly lower than when grinding, and the heating source is much larger. There is no answer to the question of the specific austenitization temperature, depending on the chemical composition of the steel.

In [12], the inverse martensitic transformation in steels, alloyed with Cr–Ni–Mo is investigated. The initial structure is tempered martensite and chromium carbides. The transformation of the initial coarse-grained structure into a fine-grained polygonal structure was studied. This is a purely metallurgical study, the results of which are difficult to apply to the question under investigation, since it is practically impossible even to artificially create conditions similar to experimental conditions when grinding.

In [13], 0.2 % C and 17 % Ni steels with a martensitic structure are investigated. Heating is performed below the austenite formation temperature, followed by compression deformation, at which dynamic recrystallization is observed. As a result, submicron grains of perlite were obtained.

In the present paper, the results of this article cannot be used, since the conditions for heating and deformation differ significantly from what takes place during grinding.

In work [14], investigations were carried out using electron microscopy of transition zones between martensite and austenite during pulsational heating of chromium-nickel alloys. It is established that these transition zones have complex structures with different phase compositions. However, the non-conformity with the heating conditions during the experiments and scarcity of experimental materials make it impossible to use the results for the case of reverse martensitic transformation during grinding.

In [15], the A–M transformation in a maraging steel is studied. The results cannot be used for grinding of hardened steels. In maraging steels, soft martensite with depleted carbon is formed during quenching. Hardening takes place with additional heat treatment.

Thus, it should be noted that in the literature no data have been found that would explain the reverse martensitic transformation when grinding hardened steels.

3. The aim and objectives of the study

The aim of the work is to establish the regularities of phase – structural transformations in the quenched surface layer of the part being ground with various mechanical and thermophysical characteristics under various grinding conditions. This will allow us to evaluate the joint effect of high-speed thermal processes during grinding and the chemical composition of the ground surface, to determine safe processing temperatures.

To achieve this goal, the following tasks were set:

– to determine the heating rates in the range of the 3rd tempering transformation when the contact temperature is lower and above the Ac_1 point;

– to determine the probability of high-speed tempering of martensite and the formation of austenite according to the martensite-perlite-austenite scheme, on the basis of which one can determine the temperatures at which an austenite is formed for various steels, depending on the chemical composition;

– to determine the limiting temperatures that do not cause thermal defects and the principles for determining the grinding conditions, which ensure that the temperature limits are not exceeded.

4. Materials and methods for studying phase-structural transformations in the surface layer of a part being ground

The peculiarities of the process of metal heating during grinding are the small dimensions of the thermal source, the considerable power of this source, which at a small size of the latter, ensures a high intensity of the heat flux and a short time of thermal action of this source on the metal.

The heating rates of grinding are estimated as 10^6–10^8 °C/s [1, 2].

In a number of cases, under such conditions, the martensite diffusion decay and the formation of pearlite structures are possible. In [16], the heating rates and temperature intervals at which the martensite diffusion decay is possible are shown (Fig. 1).

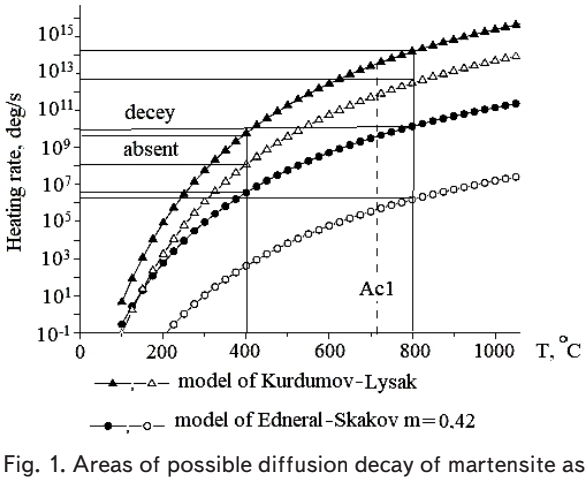

Fig. 1. Areas of possible diffusion decay of martensite as a function of the rate of heating

As can be seen from Fig. 1, while heating to around 400°C, which is typical for the temperature of the third tempering transition, the diffusion decay of martensite can occur at heating rates of $1.8 \cdot 10^6$–$1.6 \cdot 10^{10}$°C/s.

At a heating temperature of about 800°C, which is much higher than the Ac_1 point, the diffusion decay of martensite can occur at heating rates of about $1.3 \cdot 10^6$–$1.1 \cdot 10^{14}$°C/s. To determine the heating rates during grinding in the temperature range of the 3rd tempering transition at contact grinding temperatures above and below Ac_1, we use the data of [1, 2].

The curve of surface heating during grinding is described by the expression

$$T_\tau = T_{max}\left[1-\exp\left(-\frac{v_s^2\cdot\tau}{4\cdot a}\right)\right], \quad (1)$$

where T_{max} is the maximum temperature, °C; v_s is the speed of the thermal source, m/s; τ is the current time, s; a is the coefficient of thermal diffusivity of the ground material, m^2/s.

To obtain a wide range of contact temperatures, a grinding wheel of grain size 12 (E9A12SM1K6) from electrocorundum and grinding modes V_w=35 m/s, V_p=Vs=0.66 m/s, grinding depths t=0.01; 0.015; 0.02; 0.04 mm were selected. The combination of the heating curves and the steel part of the iron-carbon diagram is shown in Fig. 2.

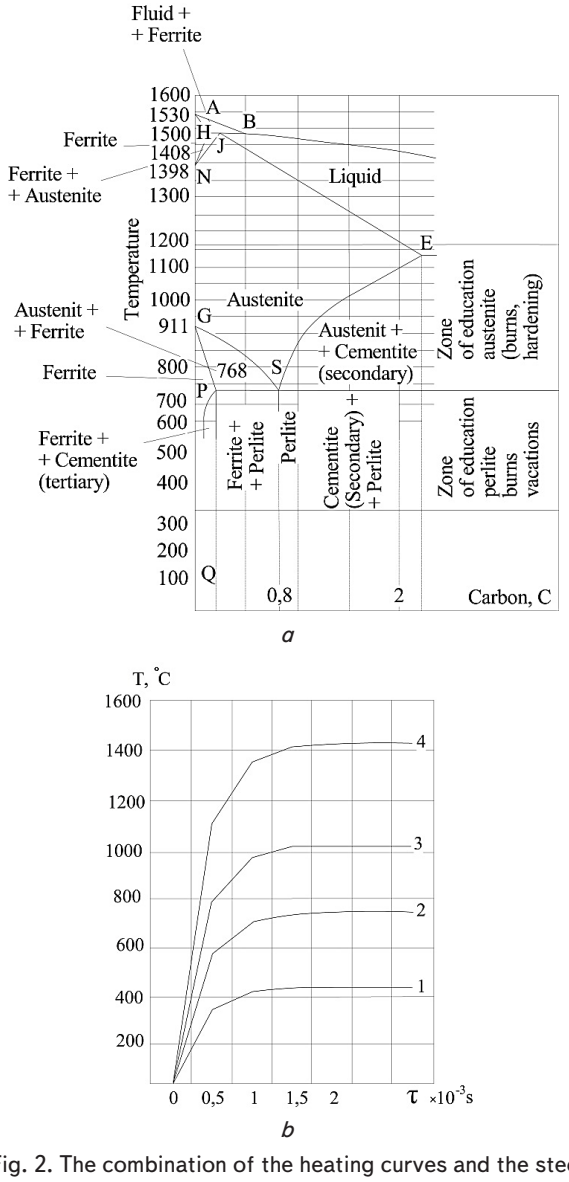

Fig. 2. The combination of the heating curves and the steel part of the diagram: *a* — iron-carbon diagram; *b* — graph of temperature growth as a function of the depth of cut

By measuring the heating rates in the temperature range from 400°C to Ac_1, the following values can be obtained: $V_4=3\cdot10^6$ °C/s; $V_3=2\cdot10^6$ °C/s; $V_2=0.3\cdot10^6$ °C/s.

By comparing the obtained values of the heating rates with the data of Fig. 1, it can be concluded that even at the maximum heating rates that may occur, during the grinding process, the diffusion decay of martensite is possible. For calculations, a very high speed of the heat source is chosen, which gives the maximum heating rates. In practice, when grinding, the speed of the heat source (the speed of the part with respect to the retarded grinding wheel) is usually smaller. Consequently, the heating rates of the surface will be somewhat lower than those shown in Fig. 2.

Thus, it can be concluded that in the overwhelming majority of cases when the hardened surface of a part is heated in the range of the temperatures of the 3rd tempering transformation and higher, the decay of the martensitic structure and the formation of austenite occurs according to the M–P–A scheme.

It should be noted that the transformation of perlite into austenite at temperatures above the GSE line can be divided into 2 stages. The first is a shear rearrangement of the BCC-FCC crystal lattice (α–γ). The second is the dissolution of carbon in the γ lattice. The timing of these events is incommensurable. According to some data, the time for rearrangement of the crystal lattice, in particular [17], is about 10^{-11} s, i. e. 0.01 ns. The time of complete dissolution of carbon in the γ lattice takes several μs or several 10^{-6} s.

The value of the austenite formation temperature above the GSE line will depend on the heating rate above this line, the carbon dissolution rate and the alloying degree of the steel.

The transformation begins with the formation of austenite grains at the ferrite-cementite interface. The resulting austenite grains initially have the same carbon concentration as ferrite, since the rate of polymorphic transformation α→γ is much higher than the rate of diffusion processes. As time elapses, due to the dissolution of carbon, the concentration in the austenite grain increases. At the end of the transformation in the austenite grain, the carbon concentration becomes uneven. In those places where cementite was present before transformation, the concentration of carbon is higher, and in those places where ferrite was present, the concentration of carbon is lower. It takes some time, depending on the temperature, to equalize the composition. The higher the temperature, the faster the diffusion process of carbon redistribution in austenite is completed. The diagram of the transformation of perlite into austenite is shown in Fig. 3, 4 [18].

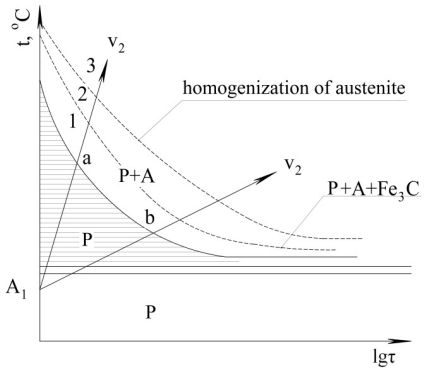

Fig. 3. The diagram of transformation of perlite into austenite

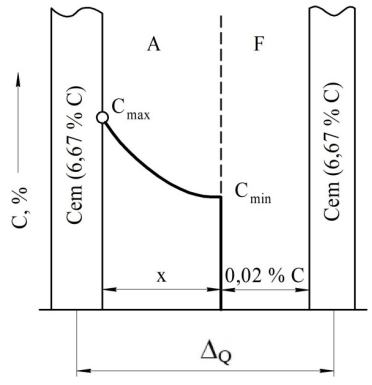

Fig. 4. Carbon distribution during the formation of austenite

For a mathematical description, we can formulate the problem in the following way: through the surface X of a semi-infinite body, the diffusion of a certain element directed into the interior of a semi-infinite body takes place. It is required to determine the concentration distribution of the diffusing element at any time.

Mathematically, the problem is formulated in the form of a differential diffusion equation (Fick's second law)

$$\frac{\partial C}{\partial \tau} = D\frac{\partial^2 C}{\partial x^2}, \tag{2}$$

Under the boundary conditions

$$\begin{aligned} &C(x,0) = C_0, \\ &C(0,\tau) = 0, \\ &\frac{\partial C(+\infty,\tau)}{\partial x} = 0, \end{aligned} \tag{3}$$

where D is the diffusion coefficient, cm^2/s; τ is the diffusion time, s; X is the coordinate; C is the concentration of the diffusing element of mass, %; C_0 is the initial concentration of the diffusing element of mass, %.

For the case of austenitic transformation, this is the concentration of carbon in the cementite.

By solving this equation by Laplace transforms, we have:

$$C_{max} = C_{max}\left|1-\Phi\left(\frac{x}{2\sqrt{D\tau}}\right)\right|, \tag{4}$$

where the second term in brackets is the integral of the Gaussian error function; x is the distance from the boundary austenite-cementite surface (Fig. 4); D is the diffusion coefficient of carbon in austenite; τ is the diffusion time.

The time of complete dissolution of carbon in the Fe_γ lattice depends on the growth rate of the austenite grain. Consequently, the time of temperature increase over Ac_1 is equal to the quotient of the linear increase in the austenite grain x and the time of complete dissolution of carbon τ:

$$V_p = \frac{x}{\tau}. \tag{5}$$

In other words, it is necessary to determine the rate of growth in a unit elementary interlamellar volume. Under these conditions, $x=\Delta_0$ (the interlamellar distance value) and $\tau=\tau_0$ (the time of completion of the process in this volume). Hence the growth rate will be:

$$V_p = \frac{\Delta_0}{\tau_0}. \quad (6)$$

By transforming the equation (4), as shown in [19], we get:

$$1-\left(\frac{C_{min}}{C_{max}}\right) = \Phi\left(0{,}5\sqrt{\frac{v_p\Delta_0}{D}}\right). \quad (7)$$

In this equation, the only unknown is the growth rate of the austenite grain. By determining V_p using the iteration method, it is possible to obtain numerical values [19], which can be interpreted by the following graph, taking into account that as a rule high-speed tempering of martensite gives fine-grained perlite with an interlamellar distance of 0.1–0.2 μm (Fig. 5).

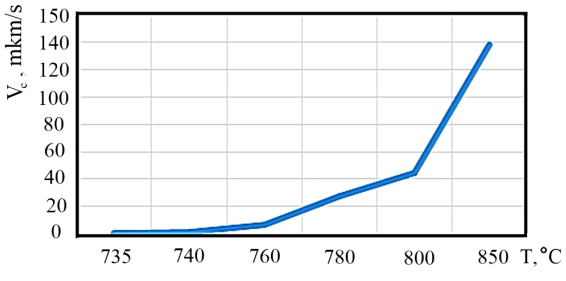

Fig. 5. The growth rate of austenite grains at various temperatures above the Ac_1 point

As can be seen from Fig. 4, the total dissolution time of carbon is the quotient of dividing the half of the interlamellar distance Δ_0 by the average grain growth rate, which from Fig. 5 is an average of 80 μm/s. Thus, the time for complete dissolution will be $0.8\cdot10^{-3}$ s. On the other hand, from Fig. 2 (curve 3), it can be determined that the average heating rate in the A_1 – 1000°C range is $0.34\cdot10^6$°C/s. During this time, the temperature above the A_1 point will rise by 272°C. Thus, the temperature of complete austenite formation is 999°C.

Such a method of determining the austenite formation temperature during grinding gives a qualitative description of the process, as it is laborious, inaccurate and not adapted to computerization. Therefore, it makes sense to approach this issue from a slightly different angle when analytical calculations are possible.

With an accuracy of ±5 %, the function Φ(y) of the equation (4) can be approximated by the expression:

$$\Phi(y) = 1 - e^{-1{,}4y^{1{,}38}}. \quad (8)$$

Then the expression (4) is transformed as follows:

$$c(x,\tau) = C_0 \exp\left[-1{,}4\left(\frac{x}{2\sqrt{Dt}}\right)^{1{,}38}\right]. \quad (9)$$

The time of complete dissolution of carbon in austenite will be:

$$\tau = \frac{x^2}{2.45D\sqrt{\left(\ln\frac{C_x}{C_0}\right)}}. \quad (10)$$

This expression in principle describes not only the diffusion time of carbon, but the diffusion time of any diffusing element in general. Therefore, knowing the diffusion coefficient and the maximum distance, this equation can be used to calculate the diffusion time of carbide and intermetallic media. The temperature at which the transformation ends is evidently equal to:

$$T_a = \tau_{tr} v_{ahr}, \quad (11)$$

where τ_{tr} is the transformation time determined by the expression (10); v_{ahr} is the average heating rate in the investigated temperature range.

The heating rate can be determined from the data of [1, 2]. For the case of dissolution of carbon in γ-iron, we get:

$$T_a = \frac{(0{,}885\Delta_0)^2 v_{heat}}{2{,}456D_\Sigma\sqrt{\left|\ln\frac{C_\gamma}{C_{cem}}\right|^3}}, \quad (12)$$

taking into account the concentration of carbon in cementite and austenite

$$T_a = \frac{(0{,}885\Delta_0)^2 v_h}{2{,}97D_\Sigma} + 727(Ac_1). \quad (13)$$

According to this expression, the heating rates and the austenite formation temperatures for various steels are calculated (Fig. 6).

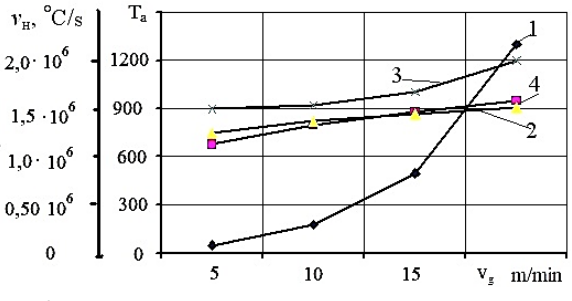

Fig. 6. Dependence of heating rates and temperatures of austenitization Ta on the speeds of the source of heating in the temperature range 727...1200°C: 1 – $v_{heating}$; 2 –45 steel; 3 – 12KH2N4A steel; 4 steel – U8

From Fig. 6 (curve 1), one can see that with an increase in the heating rate under the condition of diffusion transformation, the austenite formation temperature increases (curves 2, 3, 4). In a simplified form, this phenomenon can be explained by the fact that the $Fe_\alpha \rightarrow Fe_\gamma$ transformation occurs at the temperature of the Ac_1 point. However, it takes some time to dissolve the carbon in Fe_γ. The diffusion process of austenite formation, in particular, explains that when grinding annealed steel or steel subjected to high tempering, there are no transformations of secondary hardening. The austenite formation temperature will depend on the alloying degree of the steel and the interlamellar distance Δ_0. The greater this distance, the more time is spent on the diffusion of carbon, and the higher the temperatures of austenite formation. The formation of austenite is followed by rapid cooling at rates much higher than the critical quenching rates, especially when dealing with steels, alloyed with carbide-forming elements. A short contact time of the grinding wheel and rapid cooling, after the contact of the wheel with the given point of the metal ceased, causes certain features

of the martensitic transformation of the formed austenite. As it is well known, the increase of the carbon content and the presence of alloying elements, except for cobalt and aluminum, cause the decrease of the M_s – start and M_f –finish points of the martensitic transformation (Fig. 7) [18].

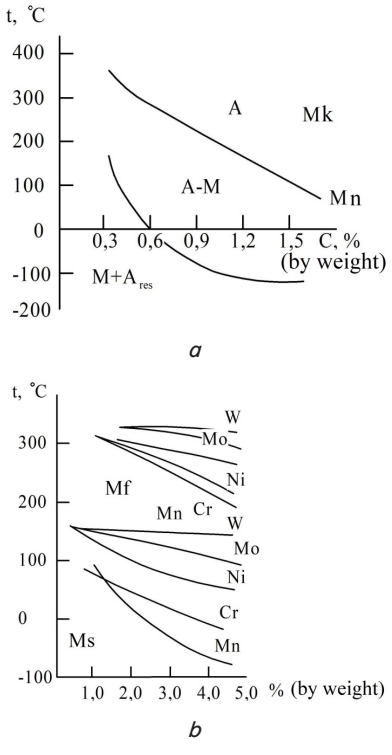

Fig. 7. Influence of the content of carbon and alloying elements on the temperature Ms and Mf martensitic points: *a* — the effect of carbon on the position of Ms and Mf; *b* — influence of alloying elements on the position of Ms and Mf

If the carbon content exceeds 0.6 %, the M_f point moves to the negative temperature range. As can be seen from Fig. 9, when cooling the austenite formed during grinding, due to high cooling rates, high degrees of supercooling are achieved.

In the A_1–M_s interval, the cooling rate is much higher than the critical quenching rates, the temperature curve is far from the C-shaped curves, so the diffusion decay of the austenite is eliminated.

The martensitic transformation region for the pre-eutectoid steels is in the range of 250...50°C [18]. Cooling in this interval at a rate of $178 \cdot 10^3$...$52 \cdot 10^3$ °C/s lasts about 0.9 ms. This cooling mode provides a high rate of martensitic transformation, which, due to its inherent kinetics, does not completely occur [19], at the end of the transformation there always remains some amount of residual austenite (Fig. 8) [18].

For eutectoid and hypereutectoid steels, the martensitic transformation interval is in the temperature range of +200...–80 °C. Since the surface is only cooled to +20 °C during grinding, the martensitic transformation interval is not completely exhausted, the formation of martensite will cease ahead of time and residual austenite will remain in the structure.

The amount of martensite formed is proportional to the fraction of the martensitic interval traversed by the temperature during cooling. When grinding cemented and quenched alloy steels, whose M_f point is in the negative temperature range, the martensitic interval does not overlap and 40–60 % of residual austenite is contained in the surface ground layer. Such a phenomenon is observed when grinding the hypereutectoid hardened SHKH15 steel.

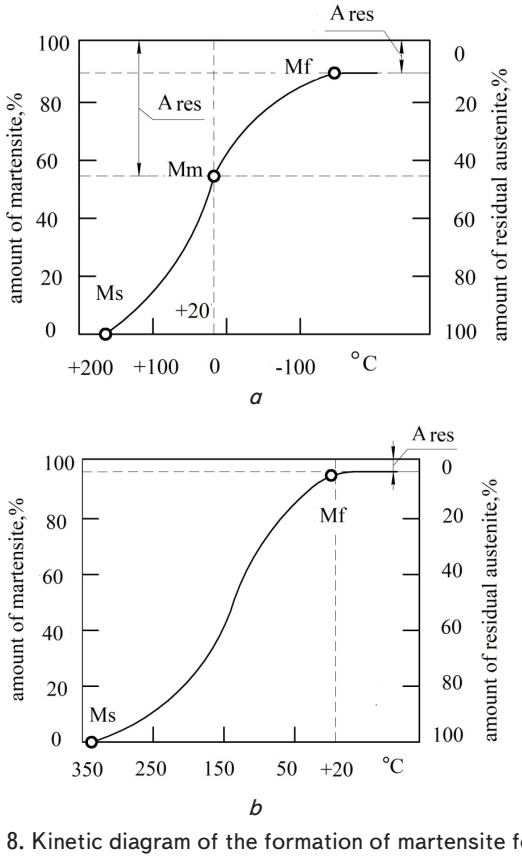

Fig. 8. Kinetic diagram of the formation of martensite for: *a* — high-carbon; *b* — medium-carbon steel

It should be noted that at a temperature above Ac_1, austenite in a thermodynamically stable state undergoes intense plastic deformation, work hardening, by cutting grains. The recrystallization temperature for such steels is about 1077°C. If the temperature of the surface is below this value, then recrystallization cannot occur at all, and if higher, then due to a small exposure it does not have time to completely occur.

Thus, when grinding conditions are created resembling high-temperature thermomechanical processing (ausforming). But because of the distorted cooling regimes, complete martensitic transformation does not occur and the residual austenite retains its work-hardened state. This state is characterized by strong distortions of the crystal lattice [7], fragmentation of the mosaic blocks, as a result of which the austenite formed in the surface layer during grinding has high hardness and brittleness.

According to the above dependences and the dependences of [20], the temperatures of the ground surface and the cooling rate are calculated.

From (8)–(13), the formation temperatures of austenite for the pre-eutectoid, eutectoid, and hypereutectoid carbonaceous and alloyed steels are determined under the processing regimes corresponding to Fig. 2 (Table 1).

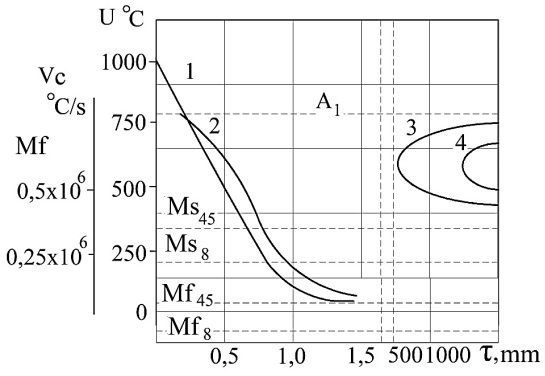

Fig. 9. Change of the surface temperature and cooling rate. Conditions of the austenitic-martensitic transformation for the pre-eutectoid and eutectoid steel: 1 — change in surface temperature; 2 — change in cooling rate; Ms_{45}, Mf_{45}, Ms_8, Mf_8 — lines of the beginning and end of the martensitic transformation, respectively, for 45 steel and U8 steel; 3, 4 — branches of the C-shaped diagram of the isothermal transformation of austenite $v_{heating\ source}$=0.15 m/s

Table 1

The temperature of the formation of austenite in the diffusion α→γ transformation under the action of the contact grinding temperature

Initial data			Ac_1			
			Steel			
V_{wheel}, m/s	V_{source} m/s	$V_{heating}$ °C/s	45 0.45 % C	U8 0.8 % C	12KH2N4A (carburizing+hardening 1.2 % C)	SHKH15 1 % C
35	0.583	3257262	797	797	870	870
45	0.75	5390	798	798	871	871
50	1.0	10353422	799	799	872	872

Note: the average heating rate $v_{heating}$, °C/s is calculated in the range of 700...1500°C

Proceeding from Table 1, it can be concluded that an increase of the carbon content and an increase in alloying degree give an increase of the austenitization temperature.

5. Discussion of the results of the investigation of martensitic transformations in the surface layer during grinding of parts from hardened steels

The combination of the surface heating curves during grinding with the steel part of the "iron-carbon" diagram shows that the temperatures above the Ac_1 line are achievable with relatively "mild" treatment regimes.

Measurement using the heating curves of heating rates shows that the values of the heating rates are such that there is a high probability of high-speed tempering of martensite and the formation of austenite according to the M–P–A scheme.

The rate of polymorphic transformation of α-γ is approximately 5 orders of magnitude higher than the rate of diffusion dissolution of carbon in Fe_γ. Therefore, after the grinding temperature corresponding to the PSK line is reached, the dissolution of carbon continues for some time during which the temperature rises. The diffusion coefficient of carbon in Fe_γ depends on the alloying elements and the concentration. Therefore, the carbon dissolution rates and, consequently, the austenite–formation temperatures are different for steels of different chemical compositions are followed by rapid cooling at rates much higher than the critical quenching rates, especially when dealing with steels, alloyed with carbide-forming elements. The amount of martensite formed is proportional to the fraction of the martensitic interval traversed by the temperature during cooling. When grinding cemented and quenched alloy steels, the M_f point of which is located in the region of negative temperatures, 40–60 % of residual austenite is very often found in the surface ground layer.

At a temperature above Ac_1, the austenite formed is subjected to intense plastic deformation – work hardening – by cutting grains.

Since the time of thermal action is very small, recrystallization either does not occur at all or is insignificant. Residual austenite retains its work-hardened state. Formed in the surface layer when grinding, it has a high hardness and brittleness.

6. Conclusions

1. The rate of surface heating during grinding in the temperature range at which the 3rd tempering transformation is possible is $3\cdot10^6$ ° C/s; – $0.3\cdot10^6$°C/s.

2. The formation of austenite in the surface layer of the part during grinding in most cases occurs due to the diffusion mechanism.

3. When austenite is formed by the diffusion mechanism at normal pressure, the Ac_1 tool point increases. This increase is the greater, the higher the heating rate.

4. The austenite formation temperature during grinding for the pre-eutectoid, eutectoid and hypereutectoid steels is in the range of 800–890 °C and tends to increase with increasing heating rate.

The austenite formed is subjected to intensive work hardening with cutting grains, and then cooled at speeds higher than the critical quenching rates. Residual austenite has a deformed crystal lattice.

When machining, the grinding temperature should not be higher than the austenite formation temperatures.

Raferences

1. Lebedev, V. G. Regularities in the formation of release fires during grinding of bearing steels [Text] / V. G. Lebedev, N. N. Klimenko // Advanced technologies and devices. – 2015. – Issue 6. – P. 35–40.
2. Lebedev, V. G. Mechanism of formation of burns during grinding of parts from hardened steels [Text] / V. G. Lebedev, N. N. Klimenko, S. A. Al-Adzhelat // Scientific notes. – 2013. – Issue 40. – P. 141–144.
3. Influence of heat generated during grinding [Electronic resource]. – Library of technical literature. – Available at: http://delta-grup.ru/bibliot/39/76.htm
4. Lobodyuk, V. A. Martensitic transformations [Text] / V. A. Lobodyuk, E. I. Estrin. – Moscow: Fizmalit, 2009. – 352 p.

5. Kremen, Z. I. Technology of grinding in mechanical engineering [Text] / Z. I. Kremen, V. G. Yuryev, A. F. Baboshkin. – Sankt-Peterburg: Polytechnic, 2015. – 424 p.
6. Fedotov, A. K. Physical Material Science. Vol. 2 [Text] / A. K. Fedotov. – Minsk: High school, 2012. – 446 p.
7. Formation of the surface layer during machining [Electronic resource]. – Encyclopedia of Mechanical Engineering XXL. – Available at: http://mash-xxl.info/info/704122/
8. Li, X. Influence of prior austenite grain size on martensite-austenite constituent and toughness in the heat affected zone of 700 MPa high strength linepipe steel [Text] / X. Li, X. Ma, S. V. Subramanian, C. Shang, R. D. K. Misra // Materials Science and Engineering: A. – 2014. – Vol. 616. – P. 141–147. doi: 10.1016/j.msea.2014.07.100
9. Rajasekhara, S. Martensite→austenite phase transformation kinetics in an ultrafine-grained metastable austenitic stainless steel [Text] / S. Rajasekhara, P. J. Ferreira // Acta Materialia. – 2011. – Vol. 59, Issue 2. – P. 738–748. doi: 10.1016/j.actamat.2010.10.012
10. Kaluba, W. J. Morphological Evolutions in Steels during Continuous Rapid Heating [Text] / W. J. Kaluba, T. Kaluba, A. Zielinska-Lipiec // Materials Science Forum. – 2007. – Vol. 539-543. – P. 4669–4674. doi: 10.4028/www.scientific.net/msf.539-543.4669
11. Tomota, Y. Reverse austenite transformation behavior in a tempered martensite low-alloy steel studied using in situ neutron diffraction [Text] / Y. Tomota, W. Gong, S. Harjo, T. Shinozaki // Scripta Materialia. – 2017. – Vol. 133. – P. 79–82. doi: 10.1016/j.scriptamat.2017.02.017
12. Bao, Y. Z. Dynamic recrystallization by rapid heating followed by compression for a 17Ni–0.2C martensite steel [Text] / Y. Z. Bao, Y. Adachi, Y. Toomine, P. G. Xu, T. Suzuki, Y. Tomota // Scripta Materialia. – 2005. – Vol. 53, Issue 12. – P. 1471–1476. doi: 10.1016/j.scriptamat.2005.08.017
13. Blinova, E. N. Structure of the Martensite–Austenite Transition Zone After a Local Pulse Heating of the Martensite [Text] / E. N. Blinova, A. M. Glezer, M. A. Libman, E. I. Estrin // Russian Physics Journal. – 2014. – Vol. 57, Issue 4. – P. 429–435. doi: 10.1007/s11182-014-0258-y
14. Viana, N. F. The variant selection in the transformation from austenite to martensite in samples of maraging-350 steel [Text] / N. F. Viana, C. dos S. Nunes, H. F. G. de Abreu // Journal of Materials Research and Technology. – 2013. – Vol. 2, Issue 4. – P. 298–302. doi: 10.1016/j.jmrt.2013.03.017
15. Mirzoev, D. A. Leave martensite in the input of rapid heating [Text] / D. A. Mirzoev, A. A. Mirzoev, P. V. Chirkov // Bulletin of SUSU. Series: Mathematics. Mechanics. Physics. – 2016. – Vol. 8, Issue 1. – P. 61–65.
16. Krainov, A. Yu. Fundamentals of heat transfer. Heat transfer through a layer of matter [Text]: textbook / A. Yu. Krainov. – Tomsk: SST, 2016. – 48 p.
17. Komarov, O. S. Material Science and Technology of Structural Materials [Text] / O. S. Komarov, V. N. Kovalevsky, L. F. Kerzhentseva, G. G. Makaeva, O. V. Khrenov, B. M. Danilko, V. E. Chigrinov. – Minsk: New knowledge, 2009. – 670 p.
18. Biront, V. S. Theory of heat treatment [Text] / V. S. Biront. – Krasnoyarsk, 2007. – 234 p.
19. Lebedev, V. Definition of the amount of heat released during metal cutting by abrasive grain and the contact temperature of the ground surface [Text] / V. Lebedev, N. Klimenko, T. Chumachenko, I. Uryadnikova, A. Ovcharenko // Eastern-European Journal of Enterprise Technologies. – 2016. – Vol. 5, Issue 7 (83). – P. 43–50. doi: 10.15587/1729-4061.2016.81207